NeuroImage: Clinical 23 (2019) 101801

Contents lists available at ScienceDirect

NeuroImage: Clinical

journal homepage: www.elsevier.com/locate/ynicl

CSF glial biomarkers YKL40 and sTREM2 are associated with longitudinal volume and diffusivity changes in cognitively unimpaired individuals

Carles Falcon[a,b,1], Gemma C. Monté-Rubio[c,1,2], Oriol Grau-Rivera[a], Marc Suárez-Calvet[a,d,e], Raquel Sánchez-Valle[c,f], Lorena Rami[c,f], Beatriz Bosch[f], Christian Haass[d,e,g], Juan Domingo Gispert[a,b,h,*], José Luis Molinuevo[a,c,f,h,i,*]

[a] Barcelonaβeta Brain Research Center (BBRC), Pasqual Maragall Foundation, Barcelona, Spain
[b] CIBER-BBN, Madrid, Spain
[c] Alzheimer's Disease and Other Cognitive Disorders Unit, Hospital Clínic, Institut d'Investigacions Biomèdiques August Pi I Sunyer (IDIBAPS), Barcelona, Spain
[d] Biomedical Center (BMC), Biochemistry, Ludwig-Maximilians-Universität München, 81377 Munich, Germany
[e] German Center for Neurodegenerative Diseases (DZNE) Munich, Munich, Germany
[f] Neurology Department, Hospital Clínic i Provincial de Barcelona, Barcelona, Spain
[g] Munich Cluster for Systems Neurology (SyNergy), Munich, Germany
[h] Universitat Pompeu Fabra, Spain
[i] CIBER Fragilidad y Envejecimiento Saludable (CIBERFES), Madrid, Spain

ARTICLE INFO

Keywords:
TREM2
YKL40
Preclinical Alzheimer's disease
Longitudinal analysis
Mean diffusivity

ABSTRACT

Cerebrospinal fluid (CSF) YKL40 and sTREM2 are astroglial and microglial activity biomarkers, respectively. We assessed whether CSF YKL40 and sTREM2 baseline levels are associated with longitudinal brain volume and diffusivity changes in cognitively unimpaired adults. Two brain MRI scans of 36 participants (57 to 78-years old, 12 male) were acquired in a 2-year interval. $A\beta_{42}$, p-tau, YKL40 and sTREM2 concentrations in CSF were determined at baseline. We calculated gray and white matter volume changes per year maps (ΔGM and ΔWM, respectively) by means of longitudinal pairwise registration, and mean diffusivity variation per year (ΔMD) by subtraction. We checked voxel-wise for associations between ΔGM, ΔWM and ΔMD and baseline CSF level of YKL40 and sTREM2 and verified to what extent these associations were modulated by age (YKL40xAGE and sTREM2xAGE interactions). We found a positive association between ΔGM and YKL40 in the left inferior parietal region and no association between sTREM2 and ΔGM. Negative associations were also observed between ΔGM and YKL40xAGE (bilateral frontal areas, left precuneus and left postcentral and supramarginal gyri) and sTREM2xAGE (bilateral temporal and frontal cortex, putamen and left middle cingulate gyrus). We found negative associations between ΔWM and YKL40xAGE (bilateral superior longitudinal fasciculus) and sTREM2xAGE (bilateral superior longitudinal fasciculus, left superior corona radiata, retrolenticular external capsule and forceps minor, among other regions) but none between ΔWM and neither YKL40 nor sTREM2. ΔMD was positively correlated with YKL40 in right orbital region and negatively with sTREM2 in left lingual gyrus and precuneus. In addition, significant associations were found between ΔMD and YKL40xAGE (tail of left hippocampus and surrounding areas and right anterior cingulate gyrus) and sTREM2xAGE (right superior temporal gyrus). Areas showing statistically significant differences were disjoint in analyses involving YKL40 and sTREM2. These results suggest that glial biomarkers exert a relevant and distinct influence in longitudinal brain macro- and microstructural changes in cognitively unimpaired adults, which appears to be modulated by age. In younger

Abbreviations: Alzheimer's disease, AD; amyloid-β, $A\beta_{42}$; amyloid-β pathology, AβP; clinical dementia rating, CDR; cerebrospinal fluid, CSF; coefficient of variation, CV; diffusion weighted images, DWI; enzyme-linked immunosorbent assay, ELISA; fractional anisotropy, FA; gray matter, GM; gray matter volume change per year, ΔGM; lumbar puncture, LP; mild cognitive impairment, MCI; mean diffusivity, MD; mean diffusivity variation per year, ΔMD; mini mental state examination, MMSE; magnetic resonance imaging, MRI; pairwise longitudinal registration, PLR; Triggering receptor expressed on myeloid cells 2, TREM2; white matter, WM; white matter volume change per year, ΔWM

* Corresponding authors.
E-mail addresses: cfalcon@barcelonabeta.org (C. Falcon), gmonte@fundacioace.org (G.C. Monté-Rubio), ograu@barcelonabeta.org (O. Grau-Rivera), msuarez@barcelonabeta.org (M. Suárez-Calvet), rsanchez@clinic.ub.es (R. Sánchez-Valle), LRAMI@clinic.cat (L. Rami), bbosch@clinic.cat (B. Bosch), christian.haass@mail03.med.uni-muenchen.de (C. Haass), jdgispert@barcelonabeta.org (J.D. Gispert), jlmolinuevo@barcelonabeta.org (J.L. Molinuevo).
[1] Both authors equally contributed to the paper.
[2] Current affiliation: Research Center and Memory Clinic, Fundació ACE, Institut Català de Neurociències Aplicades, Barcelona, Spain.

https://doi.org/10.1016/j.nicl.2019.101801
Received 12 December 2018; Received in revised form 4 March 2019; Accepted 26 March 2019
Available online 01 April 2019

subjects increased glial markers (both YKL40 and sTREM2) predict a better outcome, as indicated by a decrease in ΔGM and ΔWM and an increase in ΔMD, whereas in older subjects this association is inverted and higher levels of glial markers are associated with a poorer neuroimaging outcome.

1. Introduction

Recent neuropathological, epidemiological and genetic studies point to an early involvement of the innate immunity system in the pathological cascade that leads to Alzheimer's disease (AD) (Eikelenboom et al., 2011; Heneka et al., 2015; Suárez-calvet et al., 2017). CSF YKL40 and sTREM2 concentrations have been associated with astroglial and microglial activity along the AD *continuum*, respectively. YKL40 is a glycoprotein involved in inflammation and tissue remodeling, which has been found to be expressed by reactive astrocytes in AD (Bonneh-Barkay et al., 2010). YKL40 has been found to be elevated along the AD *continuum*, from preclinical AD (Alcolea et al., 2015a; Sutphen et al., 2015) to mild cognitive impairment (MCI) and dementia due to AD (Craig-Schapiro et al., 2010; Olsson et al., 2013; Antonell et al., 2014), compared to healthy controls. On the other hand, triggering receptor expressed on myeloid cells 2 (TREM2) is an innate immune receptor involved in phagocytosis regulation, inflammatory signaling inhibition, and cell survival promotion that is selectively expressed by microglia in the central nervous system (Takahashi et al., 2005; Ulrich et al., 2017; Mazaheri et al., 2017; Kleinberger et al., 2014; Kleinberger et al., 2017; Hickman et al., 2013). The ectodomain of TREM2 is cleaved in the cell surface, releasing a soluble fragment (sTREM2) that can be measured in cerebrospinal fluid (CSF) (Kleinberger et al., 2014; Piccio et al., 2008). Increase in sTREM2 levels in CSF have been reported along the AD *continuum* in several independent studies (Suárez-calvet et al., 2017; Heslegrave et al., 2016; Piccio et al., 2016; Suárez-Calvet et al., 2016), while one study could not reproduce these findings (Henjum et al., 2016). Both YKL40 and sTREM2 levels in CSF have been reported to be positively correlated with age, irrespective of the presence of AD pathology, and to correlate better with tau biomarkers than $A\beta_{42}$, which suggests that their main elevation occurs once neurodegeneration is already ongoing (Suárez-calvet et al., 2017; Sutphen et al., 2015; Suárez-Calvet et al., 2016).

The study of the association between CSF glial biomarkers and regional structural and diffusivity changes on magnetic resonance imaging (MRI) may contribute to understanding AD pathophysiological mechanisms. Our group has reported distinct brain structural correlates associated with YKL40 and sTREM2 levels in a cohort of subjects including healthy controls, preclinical AD, MCI due to AD and mild dementia due to AD (Gispert et al., 2016a; Gispert et al., 2016b; Gispert et al., 2017). Specifically, in patients with MCI and mild dementia, we found a non-linear (quadratic) association between YKL40 levels and gray matter (GM) volume in temporo-parietal regions, insula and cerebellum, with greater volumes being associated with intermediate YKL40 levels (Gispert et al., 2016a). We described a positive correlation between GM volume and CSF sTREM2 in patients with MCI in temporo-parietal regions, where CSF sTREM2 levels were negatively correlated with mean diffusivity, suggesting that the increase in GM volume was due to brain swelling (Gispert et al., 2016b). Our findings supported the idea that an early neuroinflammatory response is related to AD neurodegeneration. Additionally, Alcolea et al. reported a negative correlation between CSF YKL40 and cortical thickness in temporal areas in controls and MCI with abnormal CSF $A\beta_{42}$ levels (Alcolea et al., 2015b). Together, these results illustrate the dynamic nature of the structural correlates of CSF YKL40 and sTREM2 levels across AD progression and stress the need for longitudinal studies to better describe these non-linear patterns of association. In this sense, few studies have analyzed the association between neuroinflammatory biomarkers and longitudinal brain structural changes in AD (Racine et al., 2017; Sala-Llonch et al., 2017), and, to the best of our knowledge, none has evaluated the longitudinal effect of baseline sTREM2.

The aim of the current study is to test local longitudinal GM and white matter (WM) volume and mean diffusivity (MD) changes as a function of baseline CSF YKL40 and sTREM2 levels in cognitively unimpaired subjects. We hypothesized that YKL40 and sTREM2 predict longitudinal changes in GM and WM volumes and MD in several brain areas, which may be modulated by age.

2. Methods

2.1. Participants

This study was approved by the local ethics committee and all individuals gave written informed consent to participate. A sample of 40 participants (57 to 78 years old at the time of the first scan, 12 male) was recruited at the Alzheimer's disease and other cognitive disorder unit, from the Hospital Clinic de Barcelona (Barcelona, Spain). The clinical and neuropsychological examination was performed by specialized neurologists and neuropsychologists, respectively. Three subjects were excluded because of outlier values (as defined as over 2.5 standard deviations) of sTREM2 (1 subject) and YKL40 (2 subjects). Another subject was excluded due to incomplete cognitive data, leaving the final sample size to 36 subjects.

All subjects were cognitively unimpaired as defined by: Mini Mental State Examination (MMSE) scores above 24, objective cognitive performance within the normal range (above 1.5 standard deviations below the mean, taking into account age and education) in Free and Cued Selective Reminding Test (FCSRT), preserved daily living activities as measured by the Functional Activities Questionnaire, clinical dementia rating (CDR) scale score of 0, no significant psychiatric symptoms or previous neurological disease at both time points. The MMSE was also administered at follow-up visit. At inclusion, ten subjects showed $A\beta_{42}$ values below the threshold for Aβ-pathology, that was set to 500 pg/mL (Antonell et al., 2011). We treated all participants as a single group and corrected statistical analyses by baseline levels of CSF $A\beta_{42}$ and p-tau. Four DWI images were missing (1 pre, 3 post), and hence analysis of MD variations included 32 individuals. For some subjects, DWI images were slightly truncated at the cerebellum. For this reason, we do not report MD differences at the cerebellum below the temporal lobe. Demographic information and CSF biomarker values are

Table 1
Demographic characteristics. Time in years, CSF biomarker levels in pg/mL except for sTREM2 that is in arbitrary units (normalized to an internal standard). carr, carriers.

Interscan time		Age		Years school		Gender		TIV(cc)		TIV incr (cc)		*APOE-ε4*		Aβ42		ptau		logSTREM2		YKL40		MMSE	
mean	std	mean	std	mean	std	male	total	mean	std	mean	std	carr.	total	mean	std	mean	std	mean	std	mean	std	mean	std
2,2	0,4	66,5	5,5	10,9	4,1	12	36	1582	152	−1,69	1,56	6	36	687	264	55,4	16,3	−0,358	0,23	287	84	27,9	1,7

detailed in Table 1.

2.2. CSF sampling and quantification of biomarkers

CSF was collected by lumbar puncture (LP) between 9 and 12 am. Samples were processed within 1 h. $A\beta_{42}$ and p-tau levels determination was performed by enzyme-linked immunosorbent assay (ELISA) from Innogenetics (Ghent, Belgium). YKL40 levels were analyzed with the commercial ELISA MicroVue™ YKL40 EIA (Quidel Corporation, San Diego, USA), which comprises a plate coated with streptavidin and a biotinylated murine monoclonal antibody to human YKL40, an AP-conjugated rabbit polyclonal antibody to YKL40, and a chromogenic substrate. All samples were run in duplicates (mean within run CV = 5.3%). CSF samples were diluted 1:2.5 in a final volume of 150 µL to increase the upper limit of quantitation, which was of 300 ng/mL. We expected higher concentrations because of the rank of values already reported in the literature.

sTREM2 levels were measured in duplicate by an ELISA previously described using the MSD (MesoScale Discovery) Platform (Kleinberger et al., 2014). sTREM2 measurements in the current study were previously published in the context of a broader multicenter study (Suárez-Calvet et al., 2016). The mean intra-plate coefficient of variation (CV) of the ELISA was 2.9% and the inter-plate CV 12.9%. Duplicate measures with an intra-plate CV > 15% were excluded. In order to control for inter-plate variability, a dedicated CSF sample (internal standard) was loaded in all plates and all measurements were expressed in relation to the internal standard of each plate.

2.3. Image acquisition

Subjects were examined on a 3T MRI scanner (Magnetom Trio Tim, Siemens, Germany) using a high-resolution three-dimensional structural dataset (T1-weighted magnetization-prepared rapid gradient-echo, repetition time = 2300 ms, echo time = 2.98 ms, 240 slices, field of view = 256 mm; matrix size = 256 × 256; slice thickness = 1 mm) and a diffusion-weighted sequence (DWI): TR = 13,000 ms, TE = 69.1 ms, Flip Angle = 90°, 41 non-collinear directions (b = 1000 s/mm^2) and 5 non diffusion weighted (b = 0) images, voxel resolution of 1.37 × 1.37 × 2.7 mm^3 on 59 axial slices. The mean time interval between LP and baseline MRI was 41 days and ranged between 1 and 134 days. The interval between the first and second acquisition was 2.18 ± 0.39 years. MRI data were visually inspected to discard artifacts and anatomical anomalies before the analyses.

2.4. Image preprocessing of T1 images

Morphological longitudinal changes were evaluated by means of the pairwise longitudinal registration (PLR) function of SPM12 (Wellcome Trust Center for Neuroimaging; UCL, UK; http://www.fil.ion.ucl.ac.uk/spm/) as described in (Falcon et al., 2018). In short, PLR results in a pre-post average image and an image of divergences of warps, which accounts for local shrinking or expansion of the tissues. Divergence maps were divided by the interscan delay (years, one decimal) and masked into GM or WM to get GM and WM volume change per year (ΔGM and ΔWM, respectively, from now on). ΔGM and ΔWM were normalized to MNI (Montreal National Institute) using the flow fields of average image dartel normalization (Ashburner, 2007) and smoothed with an isotropic Gaussian kernel of 10 mm FWHM (full width at half maximum).

Statistical analyses were restricted on a customized common GM or WM mask obtained from the mean T1 image in MNI space. GM mask was manually edited to remove periventricular voxels, dilated one voxel to add GM partial volume voxels and completed with a basal ganglia mask to complete the thalamus and globus pallidus, partially excluded during the segmentation. WM mask was calculated in an analogous way, but without dilatation and addition of basal ganglia. As a consequence, statistical GM and WM masks had few voxels in common: inter-tissue voxels and those voxels of the basal ganglia wrongly classified as WM in the segmentation procedure. Statistical analyses were performed directly on masked ΔGM and ΔWM instead of the standard ΔGM*GM and ΔWM*WM in order to prevent analyses also reflecting potential cross-sectional intensity differences in GM and/or WM between subjects.

2.5. Image preprocessing of DWI images

Pre and post DWI images were corrected for eddy current distortions using FMRIB Software Library (FSL) package (Jenkinson et al., 2012; Manjón et al., 2013) and then denoised with the overcomplete local PCA method from (Manjón et al., 2013). MD map was obtained with DTIfit tool from FSL. Pre and post MD maps were brought to the corresponding T1 spaces by registering them to an MD-like image obtained from native GM, WM and CSF maps. The MD-like image in native T1-space was computed using the formula: 1.2*GM + WM + 2*CSF. MD pre and post images in average space were subtracted (post-pre), masked with a GM + WM mask and divided by the interscan time (in years, one decimal) to get the mean diffusivity change per year (ΔMD from this point) at each voxel of the parenchyma. The use of MD-like images instead the usual T2 ones was due to the spatial resolution of T2 scans, that were acquired in 2D for clinical review, which was insufficient to be used in the preprocessing pipeline of the other modalities. ΔMD in pre-post average space was normalized to MNI by concatenating the transformations from average to dartel template and from there to MNI and smoothed with a Gaussian kernel of 8 mm FWHM. Statistical analyses were restricted to an addition of the GM and WM masks computed during the ΔGM and ΔWM analyses.

2.6. Statistical analyses

A Shapiro-Wilk normality test was conducted on the glial CSF biomarker variables (YKL-40, p = 0.9788; sTREM2, p = 0.0002). Therefore, sTREM2 was log-transformed to obtain a normal distribution (Shapiro-Wilk normality test on log(sTREM2), p = 0.9549). From this point on, sTREM2 will refer to the logarithm of CSF sTREM2 levels. A regression analysis was performed to assess their association with age, sex, $A\beta_{42}$, p-tau and between them. Two-sided *t*-test was used to evaluate longitudinal changes in MMSE between baseline and follow-up visits in the whole group. For all statistical tests on variables, significance was considered for $p < 0.05$.

$A\beta_{42}$ was truncated at 750 pg/mL to perform statistical analyses on images. The rationale for this decision was that it could be inadequate to correlate ΔGM, ΔWM and ΔMD with high values of $A\beta_{42}$ (Fjell et al.,

Table 2
Correlation coefficients and corresponding p-values, in brackets, between main variables.

	YKL40	logSTREM2	ptau	AβP	gender
Age	0.127 (0.460)	0.0213 (0.897)	−0.0422 (0.807)	0.322 (0.055)	0.190 (0.268)
Gender	0.289 (0.087)	0.282 (0.091)	0.158 (0.359)	−0.134 (0.434)	
AβP	0.030 (0.863)	−0.054 (0.768)	0.071 (0.682)		
ptau	0.472 (0.0036)*	0.371 (0.026)*			
logSTREM2	0.525 (0.0009)**				corr_coef (p)

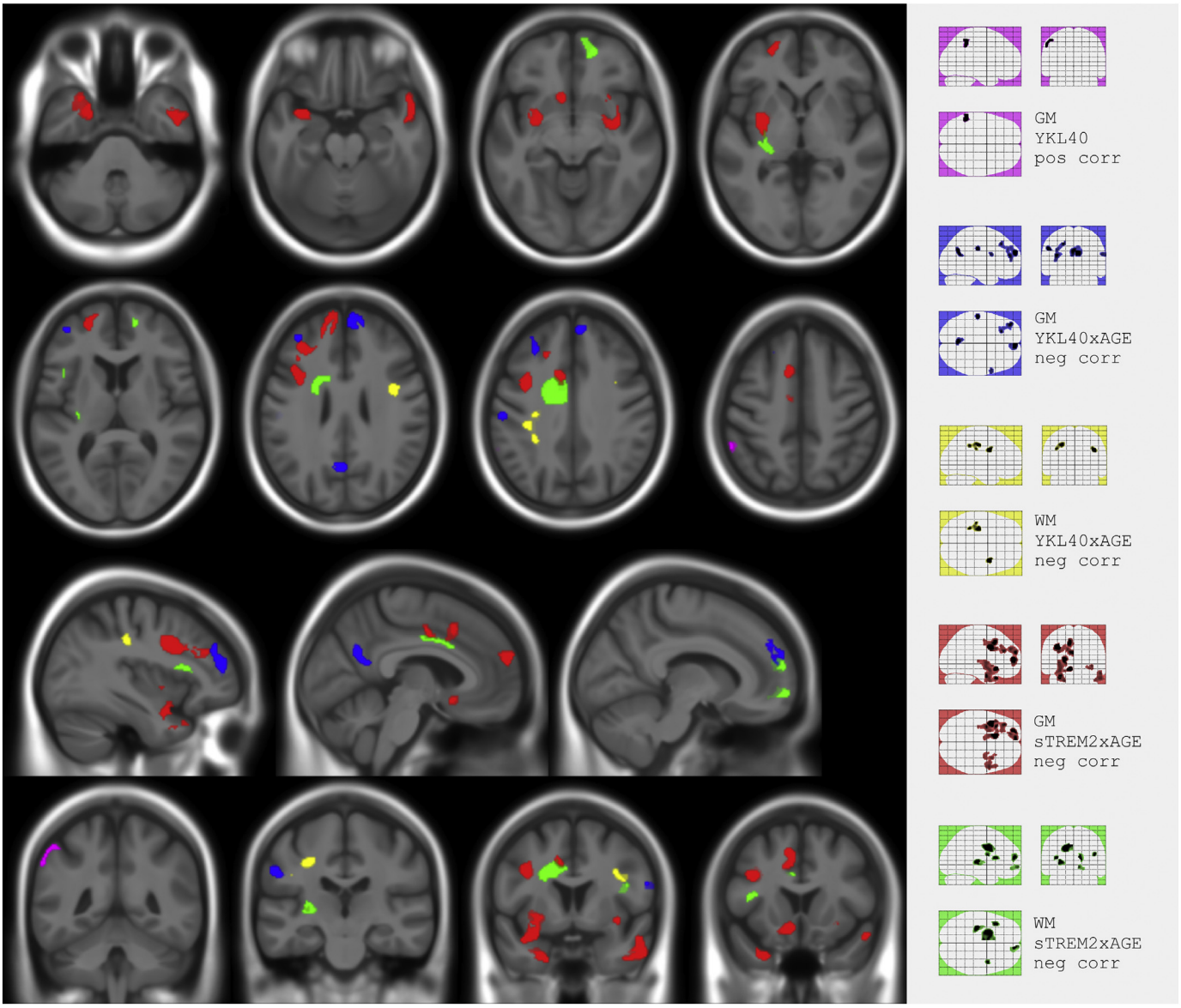

Fig. 1. Composite and glass brain maps showing significant clusters ($p < 0.001$ $k > 100$) of positive correlation between ΔGM and YKL40 (magenta) and negative correlation between: ΔGM and YKL40xAGE (blue), ΔWM and YKL40xAGE (yellow), ΔGM and sTREM2xAGE (red), and ΔWM and sTREM2xAGE (green). (For interpretation of the references to color in this figure legend, the reader is referred to the web version of this article.)

2010). The threshold of 750 pg/mL was estimated as a 20% over the threshold for pathology plus the precision of the measurement (estimated at 25% at the time the sample was analyzed (Mattsson et al., 2013), which includes the equipment accuracy and the procedures reproducibility) to ensure the absence of $A\beta_{42}$ pathology above it in any of the cases. Thus, a new variable called AβP (for $A\beta_{42}$ pathology), derived from $A\beta_{42}$ though the formula $A\beta P = \text{maximum}(1 - A\beta_{42}/750, 0)$, was used instead of $A\beta_{42}$ in subsequent imaging analyses. To illustrate this variable, Supplementary material includes a plot of AβP as a function of $A\beta_{42}$ (Fig. S1). This way, $A\beta P = 0$ meant the absence of β-amyloid pathology and the higher its value, the more severe the $A\beta_{42}$ pathology. All covariates and regressors used in imaging analyses were linearly rescaled into the [0,1] interval.

For all statistical analyses, age referred to age at the time of the first scan. We assessed the association of ΔGM, ΔWM, and ΔMD with baseline CSF YKL40 and sTREM2 levels through general linear models, as implemented in SPM12. Age, sex, $A\beta_{42}$, p-tau and the non-evaluated glial biomarker were used as covariates in all imaging analyses. Total intracranial volume (TIV) and increment of TIV, which accounted for potential miscalibrations of the scanner, since TIV is expected to be constant on time, were also included as correcting factors in ΔGM and ΔWM analyses.

Additionally, to better understand the impact of glial biomarkers on brain structural changes along time, we tested the interaction of CSF YKL40 and sTREM2 with age on ΔGM, ΔWM and ΔMD. Furthermore, we aimed to evaluate to what extent age modulated the association between glial biomarkers and longitudinal brain changes. Interactions were assumed to be multiplicative (referred to as YKL40xAGE and sTREM2xAGE from this point forward), so we checked for the association between image longitudinal changes and the product of the interacting variables correcting for them. The sign of the associations deserves special attention. In relation to volume changes and according to the divergence sign criteria, a negative association means that greater biomarker levels are associated with greater loss of volume per year; while a positive correlation indicates that higher biomarker levels are associated with lower volume changes over age. The latter may either be related to a neuroprotective effect (lower atrophy rate) or to inflammatory or compensatory changes (increased volume) (Fortea

Table 3
Locations and statistics of the clusters that overcame uncorrected $p < 0.001$; $k = 100$, between ΔGM and CSF glial biomarkers and its interaction with age. In bold result that survived a $p < 0.05$ family wise error correction at cluster level. k refers to cluster size in voxels and %cluster to the percentage of the significant cluster that belong to the aal-region. %cluster.

	GM volume change per year (ΔGM)			
	k	*Tmax*	*%cluster*	*aal label*
YKL40: pos corre	171	3,96	94,7%	Parietal Inf L
YKL40 × AGE: neg corr	535	5,45	87,9%	Frontal Sup Medial R
	335	4,83	89,9%	Precuneus L
	160	4,49	66,3%	Postcentral L
			31,3%	Supramarginal L
	602	4,30	81,9%	Frontal Mid 2 L
			16,9%	Frontal Sup 2 L
	124	3,95	75,6%	Precentral R
			27,4%	Frontal Inf Oper R
logsTREM2 × AGE: neg corr	941	5,45	44,4%	Precentral L
			23,7%	Frontal Inf Oper L
			20,1%	Frontal Mid 2 L
	264	5,43	39,2%	Rectus L
			25,0%	Caudate L
			17,8%	Olfactory L
	348	5,15	96,6%	Frontal Sup 2 L
	624	4,73	56,3%	Cingulate Mid L
			25,6%	Supp Motor Area L
	1707	**4,45**	**26,1%**	**Putamen L**
			13,7%	**Temporal Pole Mid L**
			11,5%	**Temporal Pole Sup L**
	535	4,33	57,4%	Frontal Sup Medial L
			42,6%	Frontal Sup 2 L
	732	4,12	45,0%	Temporal Mid R
			28,1%	Temporal Inf R
			13,9%	Temporal Pole Sup R
			12,8%	Temporal Pole Mid R
	264	3,91	28,8%	Putamen R

Below 10% are not reported.

Table 4
Locations and statistics of the clusters that overcame uncorrected $p < 0.001$; $k = 100$, between ΔWM and CSF glial biomarkers and its interaction with age. Regions containing less than the 10% of the cluster are not reported.

	WM volume change per year (ΔWM)		
	k	*Tmax*	*jhu label*
YKL40 × AGE: neg corr	171	4,10	Sup Long Fasc R
	466	3,89	Sup Long Fasc L
logsTREM2 × AGE: neg corr	1169	4,75	Sup Corona Radiata L
			Corpus Callosum Body L
			Cingulum L
	279	4,65	Retrolenticular Internal Capsula L
			External Capsula L
	202	4,20	Forceps Minor R
			Anterior Thalamic Radiation R
	144	4,17	Sup Long Fasc L
	116	3,90	Sup Long Fasc (temporal part) R
	185	3,78	Forceps Minor R
			Uncinate R

et al., 2010). Concerning MD, a positive association indicates that higher baseline biomarker levels predict an increase in MD and *vice versa*. In the context of AD, an increase in MD can be though as a degradation of parenchyma; whereas a decrease in MD may be due to an inflammatory process (Alexander et al., 2007). For completeness, we also run analyses on longitudinal differences in FA maps.

For all statistical tests on images, the threshold of significance was set to $p < 0.001$, uncorrected for multiple comparisons, with a minimum cluster size (k) of 100 voxels. AAL toolbox (Tzourio-Mazoyer et al., 2002) was used to label GM statistical maps. JHU track atlas on FSLeyes was used to localize significant clusters in WM (Hua et al., 2008).

3. Results

No significant intraindividual longitudinal differences in cognitive performance were found between scans. A paired *t*-test of longitudinal MMSE scores between scans showed a $p < 0.865$. Tables 1 and 2 display the demographic characteristics and CSF biomarker levels in the whole sample and the correlation coefficients (*p*-values in brackets) between main demographic variables and CSF biomarkers. Table 2 points out that CSF YKL40 and sTREM2 were significantly associated between them and with p-tau. No significant correlations were found between other variables, although there was a tendency in the association between AβP and age, and both glial biomarkers tend to be higher in men than in women.

With regard to image analyses, Fig. 1 and Tables 3 and 4, show significant clusters of associations of glial biomarkers with volume change rates. Higher YKL40 was positively associated with ΔGM in the left inferior parietal region (violet cluster). We also found a negative YKL40xAGE interaction on ΔGM in bilateral frontal areas, left precuneus and left postcentral and supramarginal gyrus (blue clusters), and a negative sTREM2xAGE interaction on ΔGM in bilateral temporal, frontal and putamen and left middle cingulate and supplementary motor area (red clusters). Regarding white matter, we found a negative YKL40xAGE interaction on ΔWM in bilateral superior longitudinal fasciculus (yellow clusters) and a negative sTREM2xAGE interaction on ΔWM in several areas including bilateral superior longitudinal fasciculus, left superior corona radiata, retrolenticular external capsule and forceps minor (green clusters).

Fig. 2 and Table 5 show significant associations with ΔMD data. YKL40 was associated with a longitudinal increase in MD in the right orbital region (green cluster). In contrast, higher sTREM2 was associated with the greater decrease in MD in the left lingual and the precuneus (red cluster). There was a positive YKL40xAGE interaction on MD involving the bilateral tail of parahippocampus and hippocampus and surrounding WM and right anterior cingulate gyrus (blue clusters), as well as a positive sTREM2xAGE interaction on ΔMD in the right superior temporal gyrus (yellow clusters). No significant cluster was found in any analysis on FA maps.

Fig. 3 shows plots of the mean value of ΔGM, ΔWM or ΔMD on different significant clusters, corrected by the reported confounders, *versus* YKL40 (first column) and sTREM2 (second column) by splitting the sample in age terciles: [56.5 to 64.2], [64.7 to 68.9], [68.9 to 78.1]. Associations in tercile subgroups were not necessarily significant. The trend line in each tercile is displayed with the only purpose of illustrating on the direction of interactions. Alternatively, Fig. S2 of Supplementary material plots the same values as a function of age by splitting the sample in YKL40 terciles: [80.2 to 241.8], [254.8 to 308.0], [310.5 to 462.28] and sTREM2 terciles: [−0.80 to −0.44], [−0.43 to −0.28] and [−0.27 to 0.20], which is mathematically equivalent. Supplementary material (Figs. S3,S4 and S5) also shows similar plots from some other significant clusters reported in Tables 3 and 4 to verify the behavior of interactions were similar in other clusters.

It is important to note that a positive or negative interaction does not mean an increase or decrease of volume. As seen in Fig. 3, most of the points in ΔGM and ΔWM plots are below zero, meaning, as expected, a loss of volume between scans in almost all cases. Similarly, the majority of points showed a positive value in ΔMD plots, indicating tissue degeneration between scans for almost all subjects. What glial CSF biomarkers modulated was the speed of such changes. The dashed line in each plot of Fig. 3, which indicated the correlation considering the whole sample, was nearly flat in all cases. This is in agreement with the fact that there were not associations with YKL40 and sTREM2 when the whole sample was considered, in those clusters.

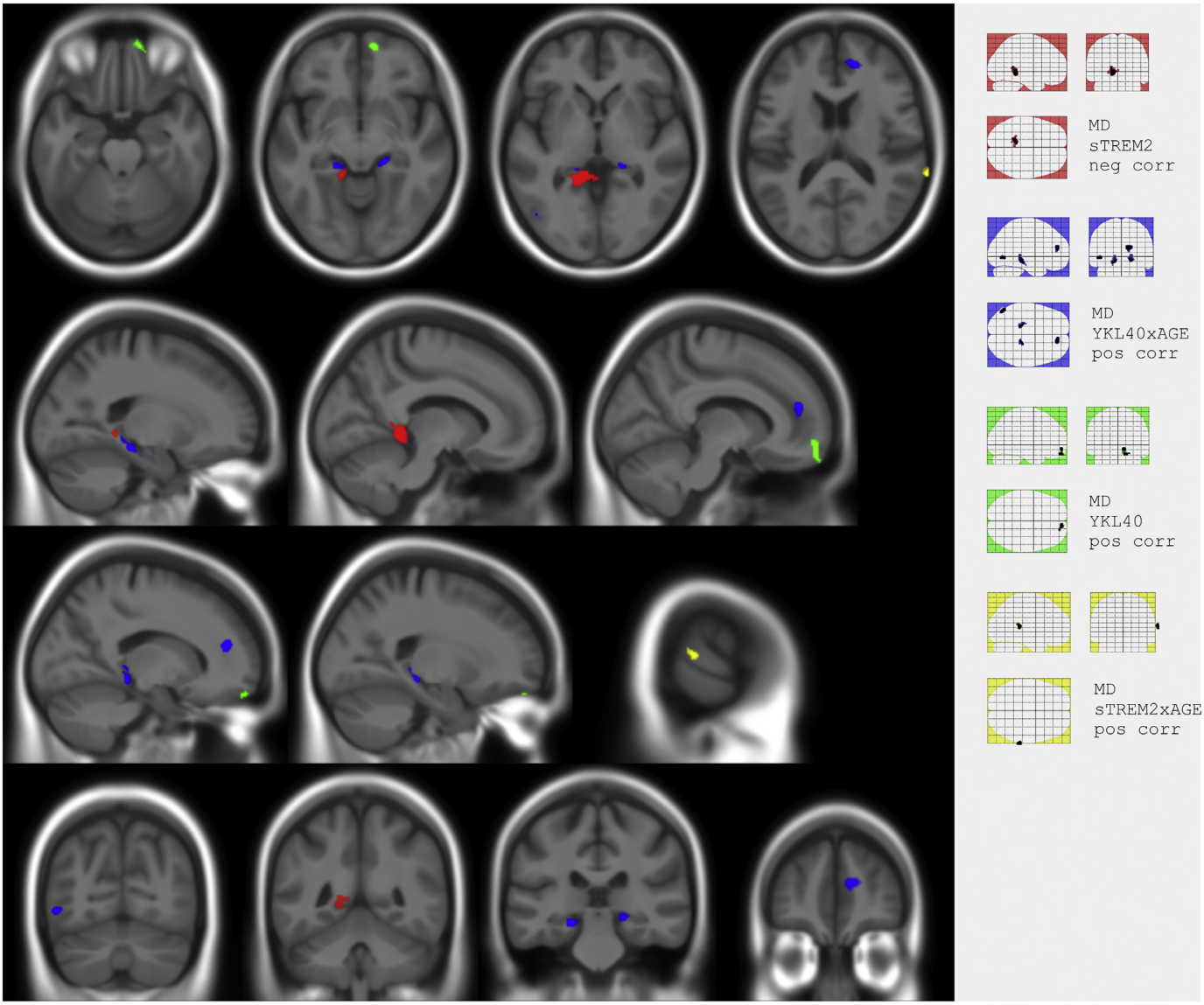

Fig. 2. Composite and glass brain maps showing significant clusters ($p < 0.001$ $k > 100$) of positive correlation between ΔMD and YKL40 (green), YKL40xAGE (blue) and sTREM2xAGE (yellow) and negative correlation between ΔMD and sTREM2 (red). (For interpretation of the references to color in this figure legend, the reader is referred to the web version of this article.)

4. Discussion

This longitudinal study investigates whether baseline CSF YKL40 and sTREM2 levels and their interaction with age predict longitudinal changes in GM, WM and MD in a sample of cognitively unimpaired adults, which includes both participants with normal and altered AD biomarkers. The main outcome of the study is the identification of longitudinal volumetric and diffusivity changes associated to baseline CSF glial markers levels in AD-related regions, previously described to undergo non-linear trajectories in association with the progression of core AD CSF biomarkers in cross-sectional studies (Gispert et al., 2016a; Fortea et al., 2011; Gispert et al., 2015). Noteworthy, baseline YKL40 and sTREM2 levels predicted longitudinal volumetric and diffusivity changes in different brain areas, despite the fact that both glial biomarkers were highly correlated. An important finding was that the association between glial markers and volumetric and diffusivity changes is modified by the effect of age. Together, our findings support the idea of an early involvement of the innate immunity in AD pathophysiology and highlight the importance of age in this immune response.

To the best of our knowledge, only two studies have previously evaluated the longitudinal brain structural correlates of CSF neuroinflammatory markers (Racine et al., 2017; Sala-Llonch et al., 2017), none of them with sTREM2. Racine et al. reported an increase in MD in the left hippocampal cingulum along time in subjects with high baseline levels of CSF YKL40, which is in line with our own findings (Racine et al., 2017). Sala-Llonch and colleagues did not find any association between baseline CSF YKL40 and longitudinal differences in cortical thickness (Sala-Llonch et al., 2017). Conversely, we found a positive association between YKL40 and ΔGM, namely high YKL40 being protective for GM loss, in the left parietal inferior lobe, where the same research group had previously described an increase in cortical thickness preceding atrophy in a genetic variant of AD (Fortea et al., 2010). Discrepancies between our study and (Sala-Llonch et al., 2017) may be due to a different sensitivity of VBM and cortical thickness to capture longitudinal structural changes (Hutton et al., 2009) and/or to demographic differences between samples (mean age of 66.5 years in this study *vs* 73.1 years in (Sala-Llonch et al., 2017)). Nir et al. reported a higher MD in late MCI than in controls in left cingulum hippocampus bundle (Nir et al., 2013), a region we reported as significant in the YKL40xAGE *vs* ΔMD association Also Gyebnaret et al. (Gyebnár et al.,

Table 5
Locations and statistics of the clusters that overcame uncorrected $p < 0.001$; $k = 100$, in the correlations between ΔMD and CSF glial biomarkers and its interaction with age. Regions containing less than the 10% of the cluster are not reported.

	MD change per year (ΔMD)				
	k	*Tmax*	*tissue*	*%cluster*	*label (aal / jhu)*
YKL40: pos corr	188	4,07	GM	39,9%	Frontal Med Orb R
			GM	27,7%	OFCmed R
			GM	13,8%	OFCant R
sTREM2: neg corr	449	5,42	GM	51,5%	Lingual L
			GM	22,1%	Precuneus L
YKL40 × AGE: pos corr	195	4,86	GM	81,5%	Cingulate Ant R
			WM	18,5%	Forceps Minor
	101	4,61	GM	49,5%	Occipital Mid L
			GM	29,7%	Occipital Inf L
			GM	13,9%	Temporal Mid L
	150	4,27	GM	48,0%	ParaHippocampal L
			GM	20,7%	Hippocampus L
			WM	23,3%	Cingulum Hippocampal L
	114	4,24	GM	46,5%	Hippocampus R
			GM	36,0%	Lingual R
			WM	10,5%	Cingulum Hippocampal R
sTREM2 × AGE: neg corr	113	4,93	GM	95,7%	Temporal Sup R

2018) reported MD differences between MCI and controls in similar areas (left precuneus, left superior frontal, right inferior temporal, left middle temporal and left supramarginal gyrus), indicating that areas we find to be associated with CSF glial biomarkers in cognitively unimpaired individuals present MD changes in posterior stages of the AD *continuum*.

Neuroimaging correlates of CSF sTREM2 have only been investigated in cross-sectional analyses. Our group described an association between higher CSF sTREM2 and higher GM volume in MCI patients, mainly occurring in temporal and parietal regions typically involved in early AD (Gispert et al., 2016b). In that work, we also reported an association between increased sTREM2 and decreased MD in bilateral temporal inferior cortex and other regions that overlapped with areas where increased GM volume was found. The regions reported in those papers on MCI almost coincide with those whose evolution has been shown to be related to CSF YKL40 and sTREM2 in this paper on cognitively unimpaired adults. Interestingly, part of the previously described areas described to be associated with CSF YKL40 in those works were related to sTREM2 or sTREM2xAGE in our study and *vice versa*. This statement together with the fact that YKL40- and sTREM2-related areas in our work were disjoint might reveal that YKL40 and sTREM2 could influence longitudinal structural changes in some brain regions at different time points in the AD *continuum*.

A key finding of the present study is the fact that the association between glial markers and volumetric and diffusivity measures are modified by age. Our findings suggest that increased glial markers YKL40 and sTREM2 in younger subjects are associated with either decreased volume change rate (*i.e.* a neuroprotective effect), an increase in brain volume (which may reflect tissue inflammation) or both, while in older subjects, increased glial markers would be associated with a deleterious effect (*i.e.* accelerated brain parenchyma loss) (Figs. 3 and S4 and S5 of Supplementary material). The pattern of MD changes across age groups is in line with this interpretation. While in younger subjects, higher basal glial markers levels predicted lower MD, which may reflect an increased cellularity (presumably caused by the proliferation of glial cells), in the older group, higher glial markers levels predicted an increase in MD, which is usually associated with parenchyma loss. These would support that volumetric changes in the younger group may be partially mediated by neuroinflammation. However, caution must be taken with regards to this statement, as the positive association between YKL40 and ΔGM observed in the inferior parietal region was not accompanied by a longitudinal MD decrease at this significance level.

With regard to the distribution of significance maps, we expected bilateral effects. Therefore, we inspected contrast images (displayed in the Supplementary material) to check whether bilateral differences were due to a lower effect (asymmetrical contrast) or to an increase of the residuals (otherwise). As can be observed in Fig. S2 (Supplementary material), contrasts for GM as well as for some WM ones, with the exception of the first (YKL40xAGE) and the highest slice of the sTREM2xAGE image, were mostly symmetric. MD maps appeared to be noisier in comparison, and while some displayed symmetrical effects (YKL40xAGE), the remaining ones did not.

The main limitation of this study was the reduced size of the longitudinal data sample. This made us use a lenient statistical threshold that increases the risk of false positives. Importantly, however, the significant clusters described herein are consistent with previous works and known to be related to CSF AD biomarkers. We are also aware that the sample might describe a particular temporal window concerning normal aging and preclinical AD changes (Falcon et al., 2018). Another potential limitation was that the time between LP and scan was not homogeneous. To check for the effect of this time range (if any) we computed *t*-test of demographic variables between two groups: 1) subjects whose time between LP and scan was > 41 days, in absolute value, and 2) the rest of subjects. The *p*-values of these *t*-tests were: Age ($p = 0.16$); Aβ42 ($p = 0.23$); p-tau ($p = 0.65$); YKL40 ($p = 0.84$); sTREM2 ($p = 0.36$). Furthermore, we also repeated the neuroimaging analyses including a categorical nuisance covariate (time between LP and scan > 41 days), resulting in minimal differences in statistical maps. Additionally, the lack of field homogeneity maps to perform a correction for echo-planar imaging distortion was a limitation in the analyses of MD. Due to this, MD maps showed high variance in the temporal poles and basal-temporal and frontal regions, which could hide some true positive associations between ΔMD and glial biomarkers in those areas. A second effect, was the requisite of using a whole parenchyma mask in MD analyses, which resulted in some tissue mixing when smoothing and increased the number of voxels in analyses penalizing correction for multiple comparisons. To apply GM or WM masks on distorted MD maps to perform an analysis of MD in GM or WM exclusively would have resulted in thousands of misclassified voxels in the frontal lobe. Another important restriction of our work was the lack of longitudinal CSF biomarker data, making impossible interesting analyses regarding the relationship between image and CSF biomarkers longitudinal changes. In particular, this prevented us from performing between-group analyses and determining the association of ΔGM, ΔWM and ΔMD with longitudinal changes of CSF biomarkers. Finally, the cerebral pattern of expression of YKL40 and sTREM2 remains to be described, as well as their association with increased glial CSF biomarkers.

5. Conclusions

We have shown that the levels of glia-related CSF biomarkers, namely sTREM2 and YKL40 predict brain longitudinal volumetric and diffusivity changes in cognitively healthy elderly. These associations mainly occurred in AD-related areas and were modulated by the effect of age. The regional patterns associated with each glial marker were disjoint, therefore suggesting that sTREM2 and YKL40 play a different role in incipient structural brain changes in cognitively normal elder people. While in younger subjects, increased glial markers (both YKL40 and sTREM2) predict a better outcome, as indicated by a decrease in ΔGM and ΔWM, in older subjects this association is inverted and higher levels of these glial markers are associated with a poorer neuroimaging outcome.

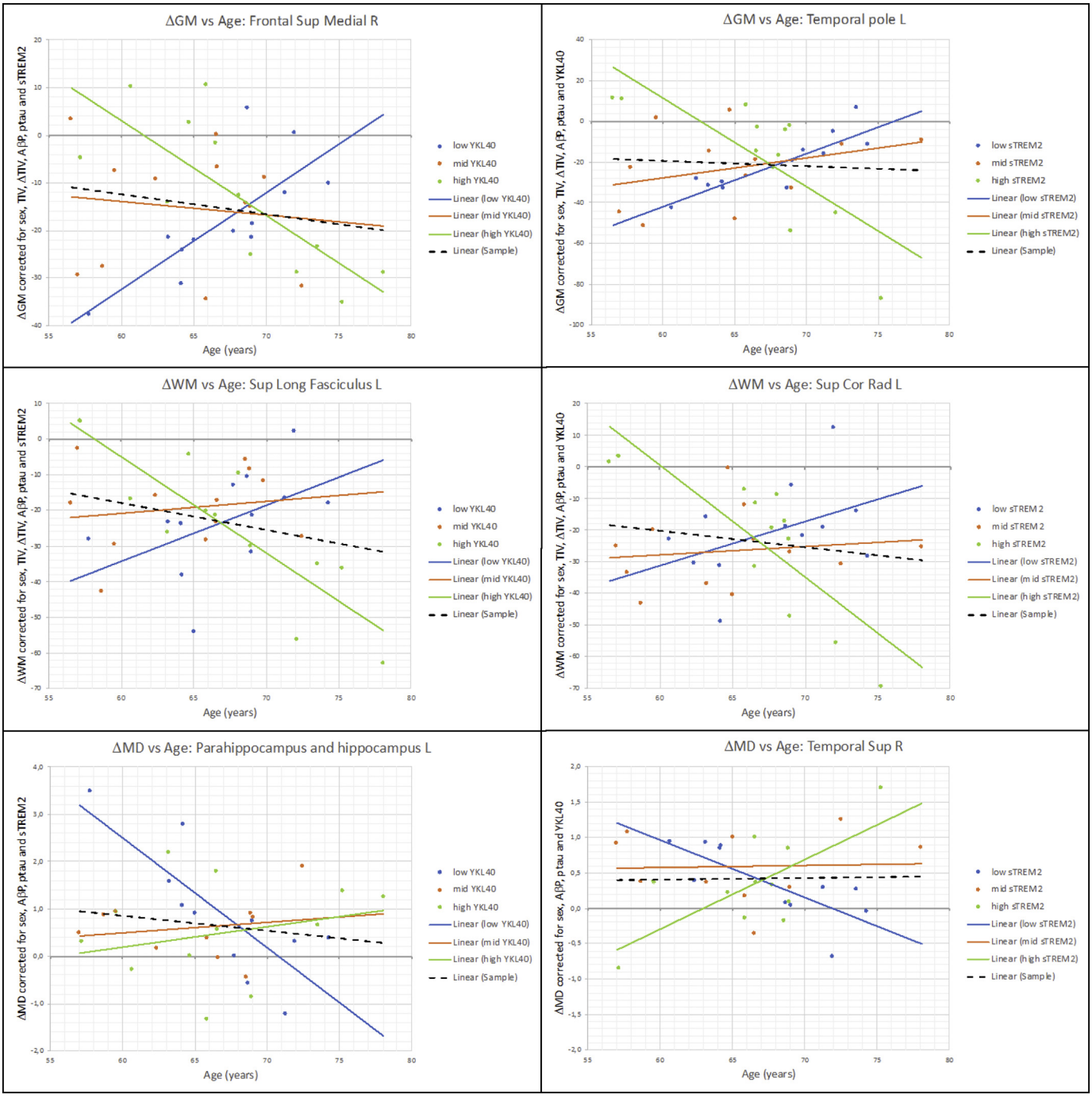

Fig. 3. Plot of corrected values of ΔGM, ΔWM and ΔMD as a function of YKL40 and sTREM2 respectively by splitting the sample into age terciles: [56.5 to 64.2], [64.7 to 68.9] and [68.9 to 78.1]. Black dash line shows the correlation considering the whole sample. Same data than Fig. S2 but in a different presentation. Just for illustrative purposes: Trend lines are not necessarily significant. The division into terciles displayed in this figure only has the purpose of.

Funding

The research leading to these results has received support from the Innovative Medicines Initiative Joint Undertaking under grant agreement n° 115568, resources of which are composed of financial contribution from the European Union's Seventh Framework Programme (FP7/2007–2013) and EFPIA companies' in-kind contribution. Juan D Gispert holds a 'Ramón y Cajal' fellowship (RYC-2013-13054) and Lorena Rami is part of the 'Programa de Investigadores del Sistema Nacional Miguel Servet II' (CPII14/00023; IP: Lorena Rami). Marc Suárez-Calvet was awarded with an AFTD Biomarkers Initiative awards from the The Association for Frontotemporal Degeneration and receives funding from the European Union's Horizon 2020 Research and Innovation Program under the Marie Sklodowska-Curie action grant agreement No 752310. This work was supported by the Deutsche Forschungsgemeinschaft (German Research Foundation) within the framework of the Munich Cluster for Systems Neurology (EXC 1010 SyNergy), Cure Alzheimer's Fund and MetLife Foundation Award (to Christian Haass). The present communication reflects the authors' view and neither IMI nor the European Union, EFPIA, or any Associated Partners are responsible for any use that may be made of the information contained herein.

Acknowledgments

We are indebted to colleagues at the Barcelonaβeta Brain Research Center and the Institut d'Investigacions Biomèdiques August Pi I Sunyer (IDIBAPS) for fruitful discussions.

Disclosure statement

None of the authors have any competing interests to report.

Appendix A. Supplementary data

Supplementary data to this article can be found online at https://doi.org/10.1016/j.nicl.2019.101801.

References

Alcolea, D., Martínez-Lage, P., Sánchez-Juan, P., Olazarán, J., Antúnez, C., Izagirre, A., Ecay-Torres, M., Estanga, A., Clerigué, M., Guisasola, M.C., Sánchez Ruiz, D., Marín Muñoz, J., Calero, M., Blesa, R., Clarimón, J., Carmona-Iragui, M., Morenas-Rodríguez, E., Rodríguez-Rodríguez, E., Vázquez Higuera, J.L., Fortea, J., Lleó, A., 2015a. Amyloid precursor protein metabolism and inflammation markers in preclinical Alzheimer disease. Neurology 85, 626–633.

Alcolea, D., Vilaplana, E., Pegueroles, J., Montal, V., Sánchez-Juan, P., González-Suárez, A., Pozueta, A., Rodríguez-Rodríguez, E., Bartrés-Faz, D., Vidal-Piñeiro, D., González-Ortiz, S., Medrano, S., Carmona-Iragui, M., Sánchez-Saudinós, M., Sala, I., Anton-Aguirre, S., Sampedro, F., Morenas-Rodríguez, E., Clarimón, J., Blesa, R., Lleó, A., Fortea, J., 2015b. Relationship between cortical thickness and cerebrospinal fluid YKL-40 in predementia stages of Alzheimer's disease. Neurobiol. Aging 36, 2018–2023.

Alexander, A.L., Lee, J.E., Lazar, M., Field, A.S., 2007. Diffusion tensor imaging of the brain. Neurotherapeutics 4, 316–329.

Antonell, A., Fortea, J., Rami, L., Bosch, B., Balasa, M., Sánchez-Valle, R., Iranzo, A., Molinuevo, J.L., Lladó, A., 2011. Different profiles of Alzheimer's disease cerebrospinal fluid biomarkers in controls and subjects with subjective memory complaints. J. Neural Transm. 118, 259–262.

Antonell, A., Mansilla, A., Rami, L., Lladó, A., Iranzo, A., Olives, J., Balasa, M., Sánchez-Valle, R., Molinuevo, J.L., 2014. Cerebrospinal fluid level of YKL-40 protein in preclinical and prodromal Alzheimer's disease. J. Alzheimers Dis. 42, 901–908.

Ashburner, J., 2007. A fast diffeomorphic image registration algorithm. Neuroimage 38, 95–113.

Bonneh-Barkay, D., Wang, G., Starkey, A., Hamilton, R.L., Wiley, C.A., 2010. In vivo CHI3L1 (YKL-40) expression in astrocytes in acute and chronic neurological diseases. J. Neuroinflammation 7, 1–8.

Craig-Schapiro, R., Perrin, R.J., Roe, C.M., Xiong, C., Carter, D., Cairns, N.J., Mintun, M.A., Peskind, E.R., Li, G., Galasko, D.R., Clark, C.M., Quinn, J.F., D'Angelo, G., Malone, J.P., Townsend, R.R., Morris, J.C., Fagan, A.M., Holtzman, D.M., 2010. YKL-40: a novel prognostic fluid biomarker for preclinical Alzheimer's disease. Biol. Psychiatry 68, 903–912.

Eikelenboom, P., Veerhuis, R., van Exel, E., Hoozemans, J.M., Rozemuller, J.M., Van Gool, A., 2011. The early involvement of the innate immunity in the pathogenesis of lateonset Alzheimers Disease: neuropathological, epidemiological and genetic evidence. Curr. Alzheimer Res. 8, 142–150.

Falcon, C., Tucholka, A., Monté-Rubio, G.C., Cacciaglia, R., Operto, G., Rami, L., Gispert, J.D., Molinuevo, J.L., 2018. Longitudinal structural cerebral changes related to core CSF biomarkers in preclinical Alzheimer's disease: a study of two independent datasets. NeuroImage Clin. 19, 190–201.

Fjell, A.M., Walhovd, K.B., Fennema-Notestine, C., McEvoy, L.K., Hagler, D.J., Holland, D., Blennow, K., Brewer, J.B., Dale, A.M., Alzheimer's Disease Neuroimaging Initiative the ADN, 2010. Brain atrophy in healthy aging is related to CSF levels of Aβ1–42. Cereb. Cortex 20, 2069–2079.

Fortea, J., Sala-Llonch, R., Bartrés-Faz, D., Bosch, B., Lladó, A., Bargalló, N., Molinuevo, J.L., Sánchez-Valle, R., 2010. Increased cortical thickness and caudate volume precede atrophy in psen1 mutation carriers. J. Alzheimers Dis. 22, 909–922.

Fortea, J., Sala-Llonch, R., Bartrés-Faz, D., Lladó, A., Solé-Padullés, C., Bosch, B., Antonell, A., Olives, J., Sanchez-Valle, R., Molinuevo, J.L., Rami, L., 2011. Cognitively preserved subjects with transitional cerebrospinal fluid ß-amyloid 1-42 values have thicker cortex in Alzheimer's disease vulnerable areas. Biol. Psychiatry 70, 183–190.

Gispert, J.D.D., Rami, L., Sánchez-Benavides, G., Falcon, C., Tucholka, A., Rojas, S., Molinuevo, J.L.L., 2015. Nonlinear cerebral atrophy patterns across the Alzheimer's disease continuum: impact of APOE4 genotype. Neurobiol. Aging 36, 2687–2701.

Gispert, J.D., Monté, G.C., Falcon, C., Tucholka, A., Rojas, S., Sánchez-Valle, R., Antonell, A., Lladó, A., Rami, L., Molinuevo, J.L., 2016a. CSF YKL-40 and pTau181 are related to different cerebral morphometric patterns in early AD. Neurobiol. Aging 38, 47–55.

Gispert, J.D., Suárez-Calvet, M., Monté, G.C., Tucholka, A., Falcon, C., Rojas, S., Rami, L., Sánchez-Valle, R., Lladó, A., Kleinberger, G., Haass, C., Molinuevo, J.L., 2016b. Cerebrospinal fluid sTREM2 levels are associated with gray matter volume increases and reduced diffusivity in early Alzheimer's disease. Alzheimers Dement. 12, 1259–1272.

Gispert, J.D., Monté, G.C., Suárez-Calvet, M., Falcon, C., Tucholka, A., Rojas, S., Rami, L., Sánchez-Valle, R., Lladó, A., Kleinberger, G., Haass, C., Molinuevo, J.L., 2017. The APOE ε4 genotype modulates CSF YKL-40 levels and their structural brain correlates in the continuum of Alzheimer's disease but not those of sTREM2. Alzheimer's Dement. Diagn. Assess. Dis. Monit. 6, 50–59.

Gyebnár, G., Szabó, Á., Sirály, E., Fodor, Z., Sákovics, A., Salacz, P., Hidasi, Z., Csibri, É., Rudas, G., Kozák, L.R., Csukly, G., 2018. What can DTI tell about early cognitive impairment? – differentiation between MCI subtypes and healthy controls by diffusion tensor imaging. Psychiatry Res. Neuroimag. 272, 46–57.

Heneka, M.T., Carson, M.J., El, Khoury J., Landreth, G.E., Brosseron, F., Feinstein, D.L., Jacobs, A.H., Wyss-Coray, T., Vitorica, J., Ransohoff, R.M., Herrup, K., Frautschy, S.A., Finsen, B., Brown, G.C., Verkhratsky, A., Yamanaka, K., Koistinaho, J., Latz, E., Halle, A., Petzold, G.C., Town, T., Morgan, D., Shinohara, M.L., Perry, V.H., Holmes, C., Bazan, N.G., Brooks, D.J., Hunot, S., Joseph, B., Deigendesch, N., Garaschuk, O., Boddeke, E., Dinarello, C.A., Breitner, J.C., Cole, G.M., Golenbock, D.T., Kummer, M.P., 2015. Neuroinflammation in Alzheimer's disease. Lancet Neurol. 14, 388–405.

Henjum, K., Almdahl, I.S., Årskog, V., Minthon, L., Hansson, O., Fladby, T., Nilsson, L.N.G., 2016. Cerebrospinal fluid soluble TREM2 in aging and Alzheimer's disease. Alzheimers Res. Ther. 8, 1–11.

Heslegrave, A., Heywood, W., Paterson, R., Magdalinou, N., Svensson, J., Johansson, P., Öhrfelt, A., Blennow, K., Hardy, J., Schott, J., Mills, K., Zetterberg, H., 2016. Increased cerebrospinal fluid soluble TREM2 concentration in Alzheimer's disease. Mol. Neurodegener. 11, 1–7.

Hickman, S.E., Kingery, N.D., Ohsumi, T.K., Borowsky, M.L., Wang, L.C., Means, T.K., El Khoury, J., 2013. The microglial sensome revealed by direct RNA sequencing. Nat. Neurosci. 16, 1896–1905.

Hua, K., Zhang, J., Wakana, S., Jiang, H., Li, X., Reich, D.S., Calabresi, P.A., Pekar, J.J., van Zijl, P.C.M., Mori, S., 2008. Tract probability maps in stereotaxic spaces: analyses of white matter anatomy and tract-specific quantification. Neuroimage 39, 336–347.

Hutton, C., Draganski, B., Ashburner, J., Weiskopf, N., 2009. A comparison between voxel-based cortical thickness and voxel-based morphometry in normal aging. Neuroimage 48, 371–380.

Jenkinson, M., Beckmann, C.F., Behrens, T.E.J.J., Woolrich, M.W., Smith, S.M., 2012. FSL. Academic Press.

Kleinberger, G., Yamanishi, Y., Suárez-Calvet, M., Czirr, E., Lohmann, E., Cuyvers, E., Struyfs, H., Pettkus, N., Wenninger-Weinzierl, A., Mazaheri, F., Tahirovic, S., Lleó, A., Alcolea, D., Fortea, J., Willem, M., Lammich, S., Molinuevo, J.L., Sánchez-Valle, R., Antonell, A., Ramirez, A., Heneka, M.T., Sleegers, K., Van Der Zee, J., Martin, J.J., Engelborghs, S., Demirtas-Tatlidede, A., Zetterberg, H., Van Broeckhoven, C., Gurvit, H., Wyss-Coray, T., Hardy, J., Colonna, M., Haass, C., 2014. TREM2 mutations implicated in neurodegeneration impair cell surface transport and phagocytosis. Sci. Transl. Med. 6.

Kleinberger, G., Brendel, M., Mracsko, E., Wefers, B., Groeneweg, L., Xiang, X., Focke, C., Deußing, M., Suárez-Calvet, M., Mazaheri, F., Parhizkar, S., Pettkus, N., Wurst, W., Feederle, R., Bartenstein, P., Mueggler, T., Arzberger, T., Knuesel, I., Rominger, A., Haass, C., 2017. The FTD-like syndrome causing TREM2 T66M mutation impairs microglia function, brain perfusion, and glucose metabolism. EMBO J. 36, 1837–1853.

Manjón, J.V., Coupé, P., Concha, L., Buades, A., Collins, D.L., Robles, M., 2013. Diffusion weighted image denoising using overcomplete local PCA. PLoS One 8.

Mattsson, N., Andreasson, U., Persson, S., Carrillo, M.C., Collins, S., Chalbot, S., Cutler, N., Dufour-Rainfray, D., Fagan, A.M., Heegaard, N.H.H., Robin Hsiung, G.Y., Hyman, B., Iqbal, K., Lachno, D.R., Lleó, A., Lewczuk, P., Molinuevo, J.L., Parchi, P., Regeniter, A., Rissman, R., Rosenmann, H., Sancesario, G., Schröder, J., Shaw, L.M., Teunissen, C.E., Trojanowski, J.Q., Vanderstichele, H., Vandijck, M., Verbeek, M.M., Zetterberg, H., Blennow, K., S a, Käser, 2013. CSF biomarker variability in the Alzheimer's Association quality control program. Alzheimers Dement. 9, 251–261.

Mazaheri, F., Snaidero, N., Kleinberger, G., Madore, C., Daria, A., Werner, G., Krasemann, S., Capell, A., Trümbach, D., Wurst, W., Brunner, B., Bultmann, S., Tahirovic, S., Kerschensteiner, M., Misgeld, T., Butovsky, O., Haass, C., 2017. TREM2 deficiency impairs chemotaxis and microglial responses to neuronal injury. EMBO Rep. 18, 1186–1198.

Nir, T.M., Jahanshad, N., Villalon-Reina, J.E., Toga, A.W., Jack, C.R., Weiner, M.W., Thompson, P.M., 2013. Effectiveness of regional DTI measures in distinguishing Alzheimer's disease, MCI, and normal aging. NeuroImage Clin. 3, 180–195.

Olsson, B., Hertze, J., Lautner, R., Zetterberg, H., Nägga, K., Höglund, K., Basun, H., Annas, P., Lannfelt, L., Andreasen, N., Minthon, L., Blennow, K., Hansson, O., 2013. Microglial markers are elevated in the prodromal phase of Alzheimer's disease and vascular dementia. J. Alzheimers Dis. 33, 45–53.

Piccio, L., Buonsanti, C., Cella, M., Tassi, I., Schmidt, R.E., Fenoglio, C., Rinker, J., Naismith, R.T., Panina-Bordignon, P., Passini, N., Galimberti, D., Scarpini, E., Colonna, M., Cross, A.H., 2008. Identification of soluble TREM-2 in the cerebrospinal fluid and its association with multiple sclerosis and CNS inflammation. Brain 131, 3081–3091.

Piccio, L., Deming, Y., Del-Águila, J.L., Ghezzi, L., Holtzman, D.M., Fagan, A.M., Fenoglio, C., Galimberti, D., Borroni, B., Cruchaga, C., 2016. Cerebrospinal fluid soluble TREM2 is higher in Alzheimer disease and associated with mutation status. Acta Neuropathol. 131, 925–933.

Racine, A.M., Merluzzi, A.P., Adluru, N., Norton, D., Koscik, R.L., Clark, L.R., Berman, S.E., Nicholas, C.R., Asthana, S., Alexander, A.L., Blennow, K., Zetterberg, H., Kim, W.H., Singh, V., Carlsson, C.M., Bendlin, B.B., Johnson, S.C., 2017. Association of longitudinal white matter degeneration and cerebrospinal fluid biomarkers of neurodegeneration, inflammation and Alzheimer's disease in late-middle-aged adults. Brain Imag. Behav. 1–12.

Sala-Llonch, R., Idland, A.V., Borza, T., Watne, L.O., Wyller, T.B., Brækhus, A., Zetterberg, H., Blennow, K., Walhovd, K.B., Fjell, A.M., 2017. Inflammation, amyloid, and

atrophy in the aging brain: relationships with longitudinal changes in cognition. J. Alzheimers Dis. 58, 829–840.
Suárez-Calvet, M., Kleinberger, G., Araque Caballero, M.Á., Brendel, M., Rominger, A., Alcolea, D., Fortea, J., Lleó, A., Blesa, R., Gispert, J.D., Sánchez-Valle, R., Antonell, A., Rami, L., Molinuevo, J.L., Brosseron, F., Traschütz, A., Heneka, M.T., Struyfs, H., Engelborghs, S., Sleegers, K., Van Broeckhoven, C., Zetterberg, H., Nellgård, B., Blennow, K., Crispin, A., Ewers, M., Haass, C., 2016. sTREM2 cerebrospinal fluid levels are a potential biomarker for microglia activity in early-stage Alzheimer's disease and associate with neuronal injury markers. EMBO Mol. Med. 8, e201506123.
Suárez-calvet, M., Araque Caballero, M.Á., Kleinberger, G., Bateman, R.J., Fagan, A.M., Morris, J.C., Levin, J., Danek, A., Ewers, M., Haass, C., 2017. Early changes in CSF sTREM2 in dominantly inherited Alzheimer's disease occur after amyloid deposition and neuronal injury. Sci. Transl. Med. 8, 1–24.
Sutphen, C.L., Jasielec, M.S., Shah, A.R., Macy, E.M., Xiong, C., Vlassenko, A.G., Benzinger, T.L.S., Stoops, E.E.J., Vanderstichele, H.M.J., Brix, B., Darby, H.D., Vandijck, M.L.J., Ladenson, J.H., Morris, J.C., Holtzman, D.M., Fagan, A.M., 2015. Longitudinal cerebrospinal fluid biomarker changes in preclinical Alzheimer disease during middle age. JAMA Neurol. 1–14.
Takahashi, K., Rochford, C.D.P., Neumann, H., 2005. Clearance of apoptotic neurons without inflammation by microglial triggering receptor expressed on myeloid cells-2. J. Exp. Med. 201, 647–657.
Tzourio-Mazoyer, N., Landeau, B., Papathanassiou, D., Crivello, F., Etard, O., Delcroix, N., Mazoyer, B., Joliot, M., 2002. Automated anatomical labeling of activations in SPM using a macroscopic anatomical parcellation of the MNI MRI single-subject brain. Neuroimage 15, 273–289.
Ulrich, J.D., Ulland, T.K., Colonna, M., Holtzman, D.M., 2017. Elucidating the role of TREM2 in Alzheimer's disease. Neuron 94, 237–248.